

# Stochastic amplitude fluctuations of bosonic dark matter and revised constraints on linear couplings

Gary P. Centers<sup>1,2</sup>, John W. Blanchard<sup>2</sup>, Jan Conrad<sup>3</sup>, Nataniel L. Figueroa<sup>1,2</sup>, Antoine Garcon<sup>1,2</sup>, Alexander V. Gramolin<sup>4</sup>, Derek F. Jackson Kimball<sup>5</sup>, Matthew Lawson<sup>2,3</sup>, Bart Pelsers<sup>3</sup>, Joseph A. Smiga<sup>1,2</sup>, Yevgeny Stadnik<sup>2</sup>, Alexander O. Sushkov<sup>4</sup>, Arne Wickenbrock<sup>1,2</sup>, Dmitry Budker<sup>1,2,6,7,\*</sup>, and Andrei Derevianko<sup>8</sup>

<sup>1</sup>*Johannes Gutenberg-Universität, Mainz 55128, Germany*

<sup>2</sup>*Helmholtz Institute, Mainz 55099, Germany*

<sup>3</sup>*Department of Physics, Stockholm University, AlbaNova, 10691 Stockholm, Sweden*

<sup>4</sup>*Department of Physics, Boston University, Boston, Massachusetts 02215, USA*

<sup>5</sup>*Department of Physics, California State University East Bay, Hayward, California 94542-3084, USA*

<sup>6</sup>*Department of Physics, University of California, Berkeley, CA 94720-7300, USA*

<sup>7</sup>*Nuclear Science Division, Lawrence Berkeley National Laboratory, Berkeley, CA 94720, USA*

<sup>8</sup>*Department of Physics, University of Nevada, Reno, Nevada 89557, USA and*

*\*Corresponding Author, Email: budker@uni-mainz.de*

(Dated: November 21, 2023)

If the dark matter is composed of virialized particles with mass  $\lesssim 10$  eV, it is well described as a classical bosonic field. This field is stochastic in nature, where the field oscillation amplitude fluctuates following a Rayleigh distribution. Most experimental searches have been in the regime  $\gtrsim \mu\text{eV}$ , where it is reasonable to assume a fixed field oscillation amplitude determined by the average local dark matter energy density. However, several direct-detection experiments are searching in the ultra-light mass regime where the dark matter field coherence time greatly exceeds the measurement time and the field oscillation amplitude is uncertain. We show that the corresponding laboratory constraints of bosonic dark matter field couplings to standard model particles are overestimated by as much as an order of magnitude.

It has been nearly ninety years since the first hints of the missing mass we label today as dark matter (DM) [1], and its composition remains one of the biggest unanswered questions in physics. A broad class of DM candidates, including scalar (dilaton and moduli [2–5]) and pseudoscalar particles (axions and axion-like particles [6–8]), can be treated as an ensemble of identical spin-0 bosons whose statistical properties are described by the Standard Halo Model (SHM) [9, 10]. During the formation of the Milky Way these DM constituents relax into the gravitational potential and obtain, in the galactic reference frame, a quasi-Maxwellian velocity distribution with a characteristic dispersion (virial) velocity  $v_{\text{vir}} \approx 10^{-3}c$  and a cut-off at the galactic escape velocity. For particle masses  $m_\phi \ll 10$  eV the average mode occupation numbers of the DM field are large enough such that it may be treated as a classical field.

Following Refs. [11, 12] we refer to such ultralight fields,  $\phi(t, \mathbf{r})$ , as Virialized Ultra-Light Fields (VULFs), which emphasizes the SHM-governed stochastic nature of such fields. The dominant oscillation frequency of these fields is their Compton frequency  $f_c = m_\phi c^2 h^{-1}$ , however there is broadening due to the SHM velocity distribution and the dispersion relation for massive nonrelativistic bosons  $f_\phi = f_c + m_\phi v^2 (2h)^{-1}$ . The field modes of different frequency and random phase interfere with one another resulting in a net field exhibiting stochastic behavior. The dephasing of the net field can be characterized by the coherence time  $\tau_c \equiv (2\pi f_c v_{\text{vir}}^2 / c^2)^{-1}$ . For this paper we ignore the possibility of small-scale

structure such as miniclusters or Bose-Einstein condensate formation [13–16] and focus only on the stochastic properties of the bosonic dark matter field.

While the stochastic properties of similar fields have been studied before, for example in the contexts of statistical radiophysics, the cosmic microwave background, and stochastic gravitational fields [17], the statistical properties of VULFs have only been explored recently. The 2-point correlation function,  $\langle \phi(t, \mathbf{r}) \phi(t', \mathbf{r}') \rangle$ , and corresponding frequency-space DM “lineshape” (power spectral density, PSD) was derived in Ref. [12], and red-erived in the axion context by the authors of Ref. [18]. References [12, 18] explicitly discuss data-analysis implications only in the regime of the total observation time  $T$  being much larger than the coherence time,  $T \gg \tau_c$ . However, investigation of the regime  $T \ll \tau_c$  has been lacking<sup>1</sup> and is becoming more relevant as experiments begin searching such regimes.

Here we focus on this regime,  $T \ll \tau_c$ , characteristic of experiments searching for ultralight (pseudo)scalars with masses  $\lesssim 10^{-14}$  eV [20–26] having field coherence times exceeding one month. This mass range is of significant interest as the lower limit on the mass of the QCD axion extends all the way to  $10^{-22}$  eV and can be further extended if it does not make up all of the DM [7]. Addi-

<sup>1</sup> The only explicit investigation of the regime  $T \ll \tau_c$  was performed in Ref. [19] where the authors clearly state the exponential distribution of the dark matter energy density and by the authors of Ref. [18] discussing sensitivity in their Appendix E.

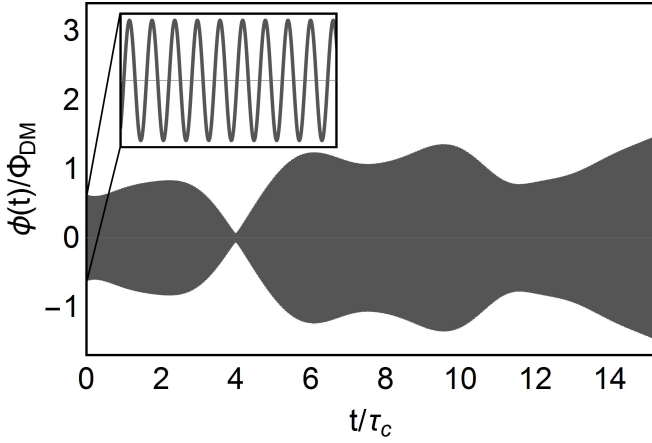


FIG. 1. VULF amplitude variation with field value  $\phi(t)$  and time rescaled by  $\Phi_{\text{DM}}$  and coherence time  $\tau_c$  respectively. The inset plot displays the high-resolution coherent oscillation starting at  $t = 0$ .

tionally, there has been recent theoretical motivation for “fuzzy dark matter” in the  $10^{-22} - 10^{-21}$  eV range [7, 27–29] and the so-called string “axiverse” extends all the way down to  $10^{-33}$  eV [30]. Similar arguments also apply to dilatons and moduli [31].

Figure 1 shows a simulated VULF field using the field PSD [12, 18], illustrating the amplitude modulation present over several coherence times. At short time scales ( $\ll \tau_c$ ) the field coherently oscillates at the Compton frequency, see the inset of Fig. 1, where the amplitude  $\Phi_0$  is fixed at a single value sampled from its distribution. An unlucky experimentalist could even have near-zero field amplitudes during the course of their measurement.

On these short time scales the DM signal  $s(t)$  exhibits a harmonic signature,

$$s(t) = \gamma\phi(t) \approx \gamma\Phi_0 \cos(2\pi f_\phi t + \theta), \quad (1)$$

where  $\gamma$  is a coupling strength to a standard-model field and  $\theta$  is a fixed but unknown phase. In this regime the amplitude  $\Phi_0$  is unknown and yields a time-averaged energy density  $\langle \phi(t)^2 \rangle_{T \ll \tau_c} = \Phi_0^2/2$ . However, for times much longer than  $\tau_c$  the energy density approaches the ensemble average determined by  $\langle \Phi_0^2 \rangle = \Phi_{\text{DM}}^2$ . This field oscillation amplitude is estimated by assuming that the average energy density in the bosonic field is equal to the local DM energy density  $\rho_{\text{DM}} \approx 0.4 \text{ GeV}/\text{cm}^3$ , and thus  $\Phi_{\text{DM}} = \hbar(m_\phi c)^{-1} \sqrt{2\rho_{\text{DM}}}$ .

The oscillation amplitude sampled at a particular time for a duration  $\ll \tau_c$  is not simply  $\Phi_{\text{DM}}$ , but rather a random variable whose sampling probability is described by a distribution characterizing the stochastic nature of the VULF. Until recently, most experimental searches have been in the  $m_\phi \gg 10^{-14}$  eV regime with short coherence times  $\tau_c \ll 1$  day. However, for smaller boson masses it becomes impractical to sample over many coherence

times: for example,  $\tau_c \gtrsim 1$  year for  $m_\phi \lesssim 10^{-17}$  eV. Assuming  $\Phi_0 = \Phi_{\text{DM}}$  neglects the stochastic nature of the bosonic dark matter field [20–25].

The field  $\phi(t)$  is a sum of different field modes with random phases. The oscillation amplitude,  $\Phi_0$ , resulting from the interference of these randomly phased oscillating fields can be visualized as arising from a random walk in the complex plane which is described by a Rayleigh distribution,

$$p(\Phi_0) = \frac{2\Phi_0}{\Phi_{\text{DM}}^2} \exp\left(-\frac{\Phi_0^2}{\Phi_{\text{DM}}^2}\right), \quad (2)$$

analogous to that of chaotic (thermal) light [32]. This distribution implies that  $\sim 63\%$  of all amplitude realizations will be below the r.m.s. value  $\Phi_{\text{DM}}$ .

We refer to the conventional approach assuming  $\Phi_0 = \Phi_{\text{DM}}$  as *deterministic* and approaches that account for the VULF amplitude fluctuations as *stochastic*. To compare these two approaches we choose a Bayesian framework and calculate the numerical factor affecting coupling constraints, allowing us to provide modified exclusion plots of previous deterministic constraints [20–25]. It is important to emphasize that different frameworks to interpret experimental data than presented here could change the magnitude of this numerical factor [33–36]. In any case, accounting for this stochastic nature will relax existing constraints as we show below.

*Implications for establishing constraints on coupling strength* — We follow the Bayesian framework [37] (see application to VULFs in Ref. [12]) to determine constraints on the coupling strength parameter  $\gamma$ . Bayesian inference utilizes prior information (such as assuming that one candidate makes up all of the DM, or conditions imposed by the SHM) to derive posterior probability distributions for given propositions or model parameters. One additional prior we assume here is that the DM signal is well below the experimental noise floor. The central quantity of interest in our case is the posterior distribution for  $\gamma$ , derived through application of the Bayes theorem,

$$p(\gamma|D, f_\phi, I) = \mathcal{C} \int p(\Phi_0|I) d\Phi_0 \int p(\theta|I) d\theta \times \mathcal{L}(D|\gamma, \Phi_0, \theta, f_\phi, I). \quad (3)$$

The left-hand side of the equality is the posterior distribution for  $\gamma$  where  $D$  is the data and the Compton frequency  $f_\phi$  is a model parameter. The likelihood  $\mathcal{L}(\dots)$  is the probability of obtaining the data  $D$  given the model and prior information  $I$ , such as those provided by the SHM, being true. In particular,  $p(\theta|I) = 1/(2\pi)$  is assumed to be a uniform distribution and  $p(\Phi_0|I)$  is the Rayleigh distribution in Eq. (2). The integrals on the right-hand side are to account for (to “marginalize over”) the unknown VULF phase  $\theta$  and amplitude  $\Phi_0$ . Finally,  $\mathcal{C}$  is the normalization constant. Here we assumed that

the prior distribution for  $\gamma$ ,  $p(\gamma, I)$ , is sufficiently broad and uniform, ensuring that the derived posterior distribution is not affected. This assumed prior is consistent with previous work [20–26].

If the posterior distribution,  $p(\gamma|D, f_\phi, I)$ , exhibits no evidence for a DM signal (no sharp peak) one can set constraints on the coupling strength  $\gamma$ . Such a constraint at the commonly employed 95% confidence level (CL) is given by

$$2 \int_0^{\gamma_{95\%}} p(\gamma|D, f_\phi, I) d\gamma = 0.95. \quad (4)$$

Note that the factor of two comes from the normalization of the derived posterior distributions below, Eqs. (5) and (6), where the coupling strength is allowed to be negative. Equation (4) is solved for  $\gamma_{95\%}$  to obtain the constraint.

The posteriors in both the deterministic and stochastic treatments are derived in the Supplementary Material. In short, the two posteriors differ due to the additional marginalization over  $\Phi_0$  for the stochastic case, seen in the first integral of Eq. (3). Assuming white noise of variance  $\sigma^2$  and a VULF DM signal well below the noise floor (current experimental regime), the posteriors are

$$p_{\text{det}}(x) = \mathcal{A} \exp(-x^2/4) I_0(x), \quad (5)$$

$$p_{\text{stoch}}(x) = \frac{\mathcal{B}}{1 + x^2/4} \exp\left(-\frac{1}{1 + x^2/4}\right). \quad (6)$$

Here  $x \equiv \gamma \times \Phi_{\text{DM}} \sqrt{N} \sigma^{-1}$ ,  $I_0(x)$  is the modified Bessel function of the first kind, and  $\mathcal{A} \approx 0.161$  and  $\mathcal{B} \approx 0.247$  are the normalization constants. The derivation relies on the discrete Fourier transform for a uniform sampling grid of  $N$  points. The assumptions of the uniform grid and white noise can be relaxed, as shown in the Supplementary Material. The resulting normalized posteriors are shown in Fig. 2.

Examination of Eqs. (5, 6) and Fig. 2 reveals that the Lorentzian-like stochastic posterior is much broader than the Gaussian-like deterministic posterior. It is clear that for the fat-tailed stochastic posterior, the integration must extend considerably further into the tail, leading to larger values of  $\gamma_{95\%}$  and thereby to weaker constraints,  $\gamma_{95\%}^{\text{stoch}} > \gamma_{95\%}^{\text{det}}$ . Explicit evaluation of Eq. (4) with the derived posteriors results in a relation between the constraints

$$\gamma_{95\%}^{\text{stoch}} \approx 10 \gamma_{95\%}^{\text{det}}, \quad (7)$$

where the numerical value of the scaling factor depends on CL, e.g. a 90% CL yields 5.73.

These results have been crosschecked via two alternative approaches. First, avoiding the use of the discrete Fourier transform, we derived approximate time-domain posteriors that hold for colored noise instruments and non-uniform sampling. This approximate approach

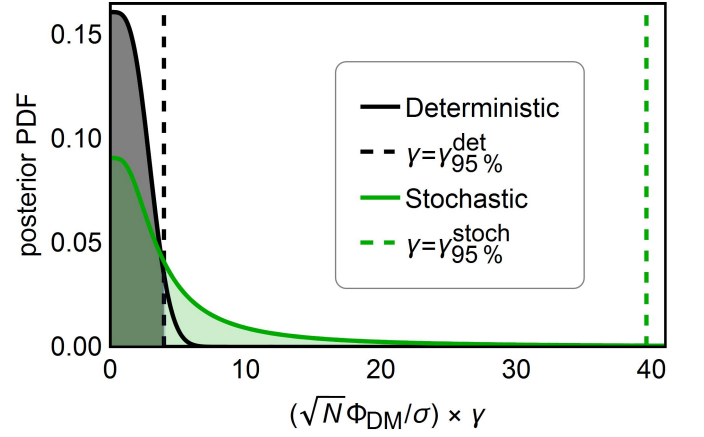


FIG. 2. Posterior distributions for the coupling strength  $\gamma$  in the deterministic and stochastic treatments, Eqs. (5) and (6) respectively. Due to the Lorentzian-like shape of the stochastic posterior one can clearly see the 95% limit is significantly larger  $\gamma_{95\%}^{\text{stoch}} / \gamma_{95\%}^{\text{det}} = 9.98$ . For the case of 90% confidence level the ratio is  $\gamma_{90\%}^{\text{stoch}} / \gamma_{90\%}^{\text{det}} = 5.73$ .

yields a result consistent with Eq. (7). Additionally, results from a Monte Carlo approach using blueice [38] to model CASPER-ZULF [21] also indicate a significant effect. Details of these alternative approaches can be found in the SM. We note that the actual value of the corrective factor may depend on the specific analysis and assumptions therein. Regardless of the chosen framework, this implies that existing constraints based on the deterministic model are overestimated by up to an order of magnitude.

*Revised exclusion plots* – As discussed earlier these ultra-light DM candidates are well motivated, and an increasing number of experiments are searching for them. Most of the experiments with published constraints thus far are haloscopes, sensitive to the local galactic DM and affected by Eq. (7). However, experiments that measure axions generated from a source, helioscopes or new force searches for example, do not fall under the assumptions made here. We illustrate how these existing constraints have been affected in Fig. 3 and provide more detailed exclusion plots for the axion-nucleon coupling  $g_{aNN}$  [20–22, 26] in Fig. 4 and for dilaton couplings [24, 25] in Fig. 5.

We have not included the higher mass regions of the published data from CASPER-ZULF-Sidebands [21] and the two isotope dysprosium spectroscopy [24], stopping when their measurement time exceeds the coherence time. How the factor shown in Eq. (7) changes in the regime where  $T \gtrsim \tau_c$  needs to be treated in more detail.

The published limits of CASPER-ZULF-Sidebands used a 90% CL, so we adjusted their data to a 95% CL for consistency using the factor determined from the ratio  $\gamma_{95\%}^{\text{stoch}} / \gamma_{90\%}^{\text{det}}$ .

*Conclusion* – We have identified the conventional, de-

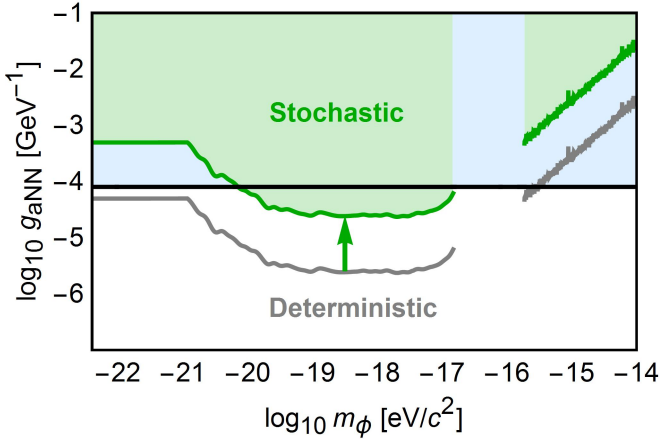


FIG. 3. Illustration of the modification to previous laboratory constraints, gray line, for the axion-nucleon coupling,  $g_{aNN}$ . The green region represents the haloscopes affected by the stochastic treatment: CASPER-ZULF-Comagnetometer [22], -Sidebands[21], and nEDM [20]. The blue region is a search for new forces using a  $K$ - $^3\text{He}$  comagnetometer [26], not sensitive to galactic dark matter.

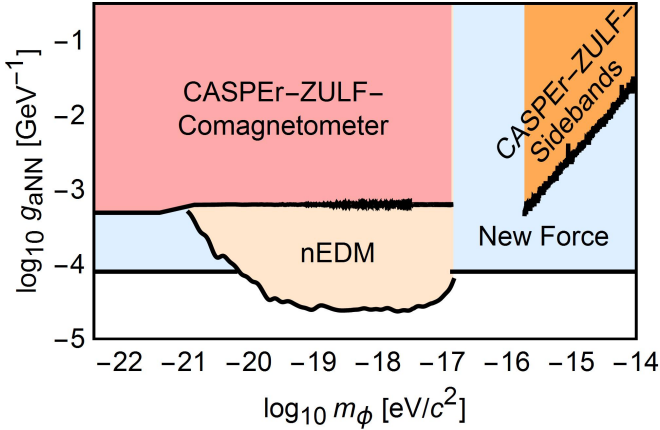


FIG. 4. An updated VULF exclusion plot of laboratory constraints for the axion-nucleon coupling,  $g_{aNN}$ , from the following experiments: CASPER-ZULF [21, 22], nEDM [20], and a new force search using a  $K$ - $^3\text{He}$  comagnetometer [26].

terministic, approach that assumes  $\Phi_{\text{DM}}$  for a coherent VULF amplitude as erroneous in the regime of measurement time  $T \ll \tau_c$ . An accurate description accounts for the Rayleigh distributed amplitude  $\Phi_0$ , where the variation is induced by the random phases of individual VULF fields. The Bayesian framework we adopted to account for this stochastic nature yields a correction of about one order of magnitude, relaxing existing VULF constraints. The results indicate the importance of treating ultralight dark matter fields as stochastic entities.

*Acknowledgments* – We thank Marina Gil Sendra and Martin Engler for their insightful discussions and suggestions. We thank N. Leefer and A. Hees for providing raw data for the published deterministic constraints. We also

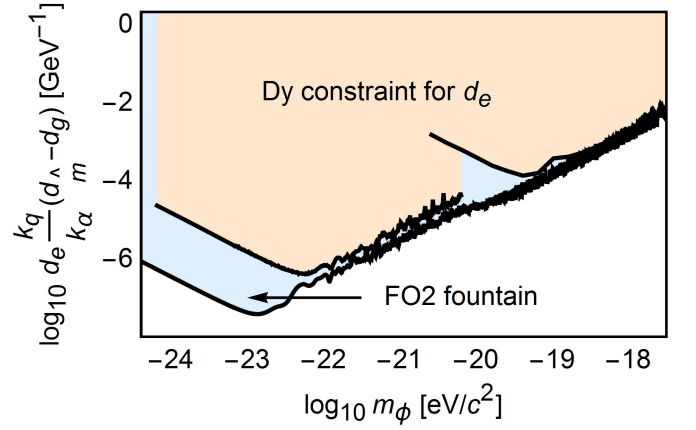


FIG. 5. An updated VULF exclusion plot of laboratory constraints for dilaton coupling strength  $d_e$  and linear combination (seen on y-axis). Details on the data for the dual rubidium and cesium cold atom fountain FO2 at LNE-SYRTE can be found in [25] and for the two isotope dysprosium spectroscopy in [24].

thank Jelle Aalbers for helpful discussions and expert advice on the blueice inference framework. Jan Conrad appreciates the support by the Knut and Alice Wallenberg Foundation. This project has received funding from the European Research Council (ERC) under the European Unions Horizon 2020 research and innovation programme (grant agreement No 695405). We acknowledge the partial support of the U.S. National Science Foundation, the Simons and Heising-Simons Foundations, and the DFG Reinhart Koselleck project.

- [1] F. Zwicky, The Redshift of Extragalactic Nebulae (Die Rotverschiebung von extragalaktischen Nebeln), Publ. Helv. Phys. Acta 10.1007/s10714-008-0707-4 (1933), arXiv:1711.01693.
- [2] S. Dimopoulos and G. F. Giudice, Macroscopic forces from supersymmetry, Physics Letters B **379**, 105 (1996).
- [3] N. Arkani-Hamed, L. Hall, D. Smith, and N. Weiner, Solving the hierarchy problem with exponentially large dimensions, Phys. Rev. D **62**, 105002 (2000).
- [4] T. R. Taylor and G. Veneziano, Dilaton couplings at large distances, Physics Letters B **213**, 450 (1988).
- [5] T. Damour and A. M. Polyakov, The string dilation and a least coupling principle, Nuclear Physics B **423**, 532 (1994).
- [6] P. W. Graham, I. G. Irastorza, S. K. Lamoreaux, A. Lindner, and K. A. van Bibber, Experimental Searches for the Axion and Axion-Like Particles, Annu. Rev. Nucl. Part. Sci. **65**, 485 (2015), arXiv:1602.00039v1.
- [7] D. J. Marsh, Axion cosmology, Phys. Rep. **643**, 1 (2016), arXiv:0610440 [astro-ph].
- [8] I. G. Irastorza and J. Redondo, New experimental approaches in the search for axion-like particles, Prog. Part. Nucl. Phys. **102**, 89 (2018).
- [9] M. Kuhlen, A. Pillepich, J. Guedes, and P. Madau, The

- Distribution of Dark Matter in the Milky Way's Disk, *The Astrophysical Journal* **784**, 161 (2014).
- [10] K. Freese, M. Lisanti, and C. Savage, Colloquium: Annual modulation of dark matter, *Reviews of Modern Physics* **85**, 1561 (2013), arXiv:1209.3339.
  - [11] A. A. Geraci and A. Derevianko, Sensitivity of atom interferometry to ultralight scalar field dark matter, *Phys. Rev. Lett.* **117**, 261301 (2016).
  - [12] A. Derevianko, Detecting dark-matter waves with a network of precision-measurement tools, *Phys. Rev. A* **97**, 042506 (2018), arXiv:1605.09717.
  - [13] P. Sikivie and Q. Yang, Bose-Einstein Condensation of Dark Matter Axions, *Phys. Rev. Lett.* **103**, 111301 (2009), arXiv:0901.1106.
  - [14] S. Davidson, Axions: Bose Einstein condensate or classical field?, *Astropart. Phys.* 10.1016/j.astropartphys.2014.12.007 (2015).
  - [15] J. Berges and J. Jaeckel, Far from equilibrium dynamics of Bose-Einstein condensation for axion dark matter, *Phys. Rev. D - Part. Fields, Gravit. Cosmol.* 10.1103/PhysRevD.91.025020 (2015).
  - [16] D. F. Jackson Kimball, D. Budker, J. Eby, M. Pospelov, S. Pustelny, T. Scholtes, Y. V. Stadnik, A. Weis, and A. Wickenbrock, Searching for axion stars and Q -balls with a terrestrial magnetometer network, *Phys. Rev. D* 10.1103/PhysRevD.97.043002 (2018).
  - [17] J. D. Romano and N. J. Cornish, Detection methods for stochastic gravitational-wave backgrounds: A unified treatment, *Living Reviews in Relativity* **20**, 1 (2017), arXiv:1608.06889.
  - [18] J. W. Foster, N. L. Rodd, and B. R. Safdi, Revealing the dark matter halo with axion direct detection, *Phys. Rev. D* **97**, 123006 (2018).
  - [19] S. Knirck, A. J. Millar, C. A. O'Hare, J. Redondo, and F. D. Steffen, Directional axion detection, *J. Cosmol. Astropart. Phys.* **2018** (11), 051, arXiv:1806.05927.
  - [20] C. Abel, N. J. Ayres, G. Ban, G. Bison, K. Bodek, V. Bondar, M. Daum, M. Fairbairn, V. V. Flambaum, P. Geltenbort, *et al.*, Search for Axionlike Dark Matter through Nuclear Spin Precession in Electric and Magnetic Fields, *Phys. Rev. X* **7**, 041034 (2017).
  - [21] A. Garcon, J. W. Blanchard, G. P. Centers, N. L. Figueroa, P. W. Graham, D. F. J. Kimball, S. Rajendran, A. O. Sushkov, Y. V. Stadnik, A. Wickenbrock, T. Wu, and D. Budker, Constraints on bosonic dark matter from ultralow-field nuclear magnetic resonance, arXiv Prepr. arXiv1902.04644 (2019), arXiv:1902.04644.
  - [22] T. Wu, J. W. Blanchard, G. P. Centers, N. L. Figueroa, A. Garcon, P. W. Graham, D. F. J. Kimball, S. Rajendran, Y. V. Stadnik, A. O. Sushkov, A. Wickenbrock, and D. Budker, Search for axionlike dark matter with a liquid-state nuclear spin comagnetometer, arXiv Prepr. arXiv1901.10843 (2019), arXiv:1901.10843.
  - [23] W. A. Terrano, E. G. Adelberger, C. A. Hagedorn, and B. R. Heckel, Constraints on axionlike dark matter with masses down to  $10^{-23}$  eV/c<sup>2</sup>, arXiv Prepr. arXiv1902.04246 (2019), arXiv:1902.04246.
  - [24] K. Van Tilburg, N. Leefer, L. Bougas, and D. Budker, Search for Ultralight Scalar Dark Matter with Atomic Spectroscopy, *Phys. Rev. Lett.* **115**, 011802 (2015), arXiv:arXiv:1503.06886v1.
  - [25] A. Hees, J. Guéna, M. Abgrall, S. Bize, and P. Wolf, Searching for an Oscillating Massive Scalar Field as a Dark Matter Candidate Using Atomic Hyperfine Frequency Comparisons, *Phys. Rev. Lett.* **117**, 061301 (2016), arXiv:1604.08514 [gr-qc].
  - [26] G. Vasilakis, J. M. Brown, T. W. Kornack, and M. V. Romalis, Limits on New Long Range Nuclear Spin-Dependent Forces Set with a K-<sup>3</sup>He Comagnetometer, *Phys. Rev. Lett.* **103**, 261801 (2009).
  - [27] W. Hu, R. Barkana, and A. Gruzinov, Fuzzy Cold Dark Matter: The Wave Properties of Ultralight Particles, *Phys. Rev. Lett.* **85**, 1158 (2000).
  - [28] D. J. Marsh and J. Silk, A model for halo formation with axion mixed dark matter, *Mon. Not. R. Astron. Soc.* 10.1093/mnras/stt2079 (2014).
  - [29] L. Hui, J. P. Ostriker, S. Tremaine, and E. Witten, Ultralight scalars as cosmological dark matter, *Phys. Rev. D* 10.1103/PhysRevD.95.043541 (2017), arXiv:1610.08297.
  - [30] A. Arvanitaki, S. Dimopoulos, S. Dubovsky, N. Kaloper, and J. March-Russell, String axiverse, *Phys. Rev. D* **81**, 123530 (2010).
  - [31] A. Arvanitaki, J. Huang, and K. Van Tilburg, Searching for dilaton dark matter with atomic clocks, *Phys. Rev. D* **91**, 015015 (2015).
  - [32] R. Loudon, *The Quantum Theory of Light*, 2nd ed. (Oxford University Press, 1983).
  - [33] R. Protassov, D. A. van Dyk, A. Connors, V. L. Kashyap, and A. Siemiginowska, Statistics, Handle with Care: Detecting Multiple Model Components with the Likelihood Ratio Test, *Astrophys. J.* **571**, 545 (2002).
  - [34] G. Cowan, K. Cranmer, E. Gross, and O. Vitells, Asymptotic formulae for likelihood-based tests of new physics, *Eur. Phys. J. C* **71**, 1 (2011).
  - [35] J. Conrad, Statistical issues in astrophysical searches for particle dark matter (2015).
  - [36] M. Tanabashi, K. Hagiwara, K. Hikasa, K. Nakamura, Y. Sumino, F. Takahashi, J. Tanaka, K. Agashe, G. Aielli, C. Amsler, *et al.*, Review of Particle Physics (2018), arXiv:0601168 [astro-ph].
  - [37] P. Gregory, *Bayesian Logical Data Analysis for the Physical Sciences: A Comparative Approach with Mathematica Support* (Cambridge University Press, 2010).
  - [38] J. Aalbers, K. Dundas Moră, and B. Pelsers, JelleAalbers/blueice: v1.0.0-beta.2 (2019).

## Supplementary material



## I. CALCULATING THE EXCLUSION PLOT REVISION FACTOR

### A. Setup

The ultralight dark matter fields are composed of a large number of individual modes with randomized phases. As such, due to the central-limit theorem, the VULF fields belong to a broad class of Gaussian random fields, encountered in many subfields of physics. The statistical properties of such fields are fully described by the two-point correlation functions in time domain or power-spectral densities in frequency space, see VULF-specific discussion in Ref. [1].

Here we consider an ultralight dark matter search in the regime when the observation time  $T$  is shorter than the coherence time  $\tau_c$  of dark matter field. Because on this short time scales the VULF oscillations are nearly coherent, the data streams are fitted to an oscillating signal

$$s(t) = \gamma \phi(t) = \gamma \Phi_0 \cos(2\pi f_\phi t + \theta). \quad (1)$$

Here  $f_\phi$  is the field Compton frequency (specific to particular realization as the frequency can be Doppler shifted),  $\theta$  is an unknown yet fixed phase, and  $\gamma$  is a coupling strength that is to be constrained. We fix the amplitude of the DM field to be positive,  $\Phi_0 \geq 0$  and the phase  $\theta$  of the field to lie in the range  $[0 - 2\pi)$ . The coupling strength  $\gamma$  can have an arbitrary sign.

In the conventional (and as we show erroneous) approach the DM field amplitude  $\Phi_0$  is fixed to its root-mean-square value  $\Phi_{\text{DM}}$ , defined in the main body of the paper. We refer to such an approach as *deterministic*. The key issue is that for a given experimental run  $T \ll \tau_c$ , the value of the DM field amplitude  $\Phi_0$  can substantially differ from  $\Phi_{\text{DM}}$ ; the amplitude is a random variable. This is apparent from the simulation presented in Fig. 1 of the main text. Thus  $\Phi_0$  has to be treated as a marginalization parameter in the analysis. We refer to this treatment as *stochastic*. This has important implications for establishing constraints on  $\gamma$ .

The probability densities for the DM field amplitude in the two approaches can be summarized as

$$p(\Phi_0|\Phi_{\text{DM}}) = \begin{cases} \delta(\Phi_0 - \Phi_{\text{DM}}), & \text{deterministic} \\ \frac{2\Phi_0}{\Phi_{\text{DM}}^2} \exp\left(-\frac{\Phi_0^2}{\Phi_{\text{DM}}^2}\right), & \text{stochastic} \end{cases} \quad (2)$$

The stochastic probability distribution for the amplitude can be recast into probability distribution for the local energy density  $\rho = \Phi_0^2 f_c^2 / 2$  of dark matter field,

$$p(\rho|\rho_{\text{DM}})d\rho = \frac{1}{\rho_{\text{DM}}} e^{-\rho/\rho_{\text{DM}}} d\rho, \quad (3)$$

in agreement with Ref. [2].

Below, we show that for a fixed value of  $\Phi_0 = \Phi_{\text{DM}}$  the posterior distribution for  $\gamma$  is Gaussian-like, dropping exponentially for large values of  $\gamma$ . Then, we allow  $\Phi_0$  to be a random variable with a probability distribution dictated by the standard halo model. In this stochastic treatment, we show that the poster distribution for  $\gamma$  is Lorentzian-like, with a fat  $1/\gamma^2$  tail.

The shape of the posterior distribution  $p(\gamma)$  has immediate implications for placing constraints. We will assume that the dark matter signal is well below the detection threshold, an assumption consistent with current experimental results. Then the most likely value of  $\gamma$  is zero and a constraint at say 95% confidence level,  $\gamma_{95\%}$ , can be determined from

$$2 \int_0^{\gamma_{95\%}} p(\gamma) d\gamma = 0.95. \quad (4)$$

Since the limits on  $\gamma$  are derived by integrating the posterior distribution, the integration must proceed to larger values of  $\gamma$  for the fat-tailed distribution. This leads to substantially different 95% C.L. limits on  $\gamma$  in the two treatments.

In the following, we derive the coupling-strength posteriors using three different methods: discrete Fourier transform, time-domain analysis, and calculate the scaling factor using a Monte Carlo approach with blueice [3].

### B. Derivation of coupling-strength posteriors using discrete Fourier transform

As an analytically treatable case, we assume that the data stream was acquired on a uniform time grid. Considering the oscillating nature of the signal (1), we will work in frequency space, applying discrete Fourier transform (DFT) to the data. The data set is assumed to include  $N$  measurements, taken over the total observation time  $T$ . To make the

derivation as transparent as possible, we assume that the intrinsic instrument noise is white with variance  $\sigma^2$ . The assumption of white noise, however, is hardly necessary, and the derivation remains valid for the more general case of colored noise. The generalization can be accomplished by replacing  $N\sigma^2$  with the noise power spectral density  $\tilde{S}(f_p)$ . We use DFT notation and definitions of Ref. [1] (see appendix of that paper for a review of Bayesian statistics in frequency space).

Suppose we would like to establish constraints on the coupling strength  $\gamma$  at one of the DFT frequencies  $f_p = f_c$ . If  $\tilde{d}_p$  is the DFT amplitude of the original data, the likelihood at  $f_p$  is given by

$$\mathcal{L}(\tilde{d}_p|\Phi_0, \gamma, \phi) = \frac{1}{\pi N\sigma^2} \exp\left\{-\frac{|\tilde{d}_p - \tilde{s}_p|^2}{N\sigma^2}\right\}, \quad (5)$$

where  $\tilde{s}_p = N\gamma\Phi_0 e^{i\theta}/2$  is the DFT amplitude of the signal (1). Marginalizing over phase  $\theta$  with a uniform prior (see Eq.(3) of the main text), we arrive at the phaseless likelihood

$$\mathcal{L}(\tilde{d}_p|\Phi_0, \gamma) = \frac{1}{\pi N\sigma^2} e^{-\frac{|\tilde{d}_p|^2}{N\sigma^2}} \exp\left(-\frac{N\gamma^2\Phi_0^2}{4\sigma^2}\right) I_0\left(\frac{\gamma\Phi_0|\tilde{d}_p|}{\sigma^2}\right), \quad (6)$$

where  $I_0$  is the modified Bessel function of the first kind. This type of Rice-like distribution has been derived earlier, see, e.g., Eq. (10) of Ref. [4].

According to the Bayes theorem, the posterior distribution  $p(\gamma|\tilde{d}_p, \Phi_0)$  for coupling strength  $\gamma$  is proportional to the likelihood  $\mathcal{L}(\tilde{d}_p|\Phi_0, \gamma)$ ,

$$p(\gamma|\tilde{d}_p, \Phi_0) = \mathcal{C} \exp\left(-\frac{N\gamma^2\Phi_0^2}{4\sigma^2}\right) I_0\left(\frac{\gamma\Phi_0|\tilde{d}_p|}{\sigma^2}\right), \quad (7)$$

with  $\mathcal{C}$  being the normalization constant[5]. This means that, given the data, we can explicitly construct probability distribution for the coupling strength  $\gamma$ . Since we are focusing on establishing constraints, we will assume that the DM signal is well below the detection threshold and we fix  $|\tilde{d}_p|^2$  at its average value of  $N\sigma^2$ ,

$$p(\gamma|\Phi_0) = \mathcal{C} \exp\left(-\frac{N\gamma^2\Phi_0^2}{4\sigma^2}\right) I_0\left(\frac{\sqrt{N}\gamma\Phi_0}{\sigma}\right). \quad (8)$$

The posterior depends on the assumed value of DM field amplitude  $\Phi_0$ . In the deterministic treatment,  $\Phi_0 \equiv \Phi_{\text{DM}}$ , thus  $p_{\text{det}}(\gamma) = p(\gamma|\Phi_0 \equiv \Phi_{\text{DM}})$ . This leads to the “deterministic” posterior

$$p_{\text{det}}(\gamma) = \mathcal{C} \exp\left(-\frac{N\gamma^2\Phi_{\text{DM}}^2}{4\sigma^2}\right) I_0\left(\frac{\sqrt{N}\gamma\Phi_{\text{DM}}}{\sigma}\right), \quad (9)$$

shown in Fig. 2 of the main text. Numerical integration, Eq. (4), of the posterior yields the 95% C.L. constraint

$$\gamma_{95\%}^{\text{det}} \approx 3.95 \frac{\sigma}{\sqrt{N}} \Phi_{\text{DM}}^{-1}. \quad (10)$$

As we show below, this “deterministic” constraint is off by an order of magnitude.

Now we would like to take into account that the field amplitude  $\Phi_0$  for a given experimental run is uncertain. This can be done formally by marginalizing over the field amplitudes with the Rayleigh distribution,

$$p_{\text{stoch}}(\gamma) = \int_0^\infty p(\Phi_0|\Phi_{\text{DM}}) p(\gamma|\Phi_0) d\Phi_0.$$

The result is

$$p_{\text{stoch}}(\gamma) = \frac{\mathcal{C}'}{1 + \gamma^2\Phi_{\text{DM}}^2 N/(4\sigma^2)} \exp\left(-\frac{1}{1 + \gamma^2\Phi_{\text{DM}}^2 N/(4\sigma^2)}\right), \quad (11)$$

where  $\mathcal{C}'$  is a normalization constant. Again we fixed  $|\tilde{d}_p|^2$  at its average value of  $N\sigma^2$ .



Below we will also give an alternative derivation of this posterior using the two-point correlation function for DM fields that avoids introduction of the Rayleigh distribution.

A comparison of the two resulting posteriors in deterministic and stochastic approaches is given in Fig. 2 of the main text. It is apparent that the stochastic distribution is wider. While the deterministic posterior is Gaussian-like, the stochastic posterior exhibits a Lorentzian-like character.

Now with the posterior distribution in hand, we use Eq. (4) to derive the 95% C.L. constraint

$$\gamma_{95\%}^{\text{stoch}} \approx 39.4 \frac{\sigma}{\sqrt{N}} \Phi_{\text{DM}}^{-1}. \quad (12)$$

Comparing this result with Eq. (10) derived in the deterministic treatment, we find

$$\gamma_{95\%}^{\text{stoch}} \approx 10 \gamma_{95\%}^{\text{det}}. \quad (13)$$

The exact value of the scaling factor depends on the confidence level. In any case, the stochastic constraint is always weaker than the deterministic one due to the stochastic distribution being fat-tailed, decaying only as  $\gamma^{-2}$  for large  $\gamma$ . The relation (13) immediately implies that the constraints derived in the “deterministic” approach are overestimated by an order of magnitude. This conclusion does not depend on the assumed white noise model, as in all the formulas one can simply replace  $N\sigma^2$  with the power spectral density  $\tilde{S}(f_p)$  for a specific measurement apparatus. This replacement does not modify the relation (13) between the stochastic and deterministic constraints.

Finally, we re-derive the stochastic posterior (11) starting directly from the stochastic likelihood in the frequency space. This approach avoids explicit introduction of the Rayleigh distribution of the field amplitude. The relevant likelihood at DFT frequency  $f_p$  is given by (see, e.g., [1])

$$\mathcal{L}_{\text{stoch}}(\tilde{d}_p|\gamma) = \frac{1}{\pi \Sigma_p} e^{-\frac{|\tilde{d}_p|^2}{\Sigma_p}}, \quad (14)$$

with  $\Sigma_p$  being a combined power spectral density of the device noise  $N\sigma^2$  and DM signal  $\gamma^2 \langle |\tilde{\phi}_p|^2 \rangle$ .

We compute  $\tilde{g}_p = \langle |\tilde{\phi}_p|^2 \rangle$  using the Wiener-Khinchin theorem. To this end we require the DM field auto-correlation function  $g(\tau) = \langle \phi(t)\phi(t+\tau) \rangle$ . This function was computed in [1] using SHM priors. In the relevant limit of  $\tau \ll \tau_c$  it reads

$$g(\tau) = \frac{1}{2} \Phi_{\text{DM}}^2 \cos(2\pi f_c \tau), \quad (15)$$

corresponding to a coherent oscillation at the Compton frequency. There is an important subtlety in applying the Wiener-Khinchin theorem in the limit of  $T \ll \tau_c$ , as this theorem is usually stated in the opposite limit. The exact relation between the power spectral density and the auto-covariance functions in DFT reads (see, e.g., [1])

$$\tilde{g}_p = N g(0) + 2 \sum_{l=1}^{N-1} (N-l) g\left(\frac{T}{N} l\right) \cos\left(\frac{2\pi}{N} p l\right), \quad (16)$$

leading to the PSD at the target Compton frequency ( $N \gg 1$ ),

$$\tilde{g}_p = \Phi_{\text{DM}}^2 \frac{N^2}{4}. \quad (17)$$

Returning to the likelihood of the stochastic signal (14), the combined PSD reads,

$$\Sigma_p = N\sigma^2 + \gamma^2 \tilde{g}_p = N\sigma^2 + \gamma^2 \Phi_{\text{DM}}^2 \frac{N^2}{4}.$$

Plugging  $\Sigma_p$  into the stochastic likelihood (14) and using the Bayes theorem immediately yields the stochastic posterior (11). Notice that the Lorentzian-like shape of the stochastic posterior is entirely due to the normalization pre-factor in the Gaussian likelihood (14).

### C. Approximate time-domain analysis

The results above can be also obtained in approximate way, without alluding to the DFT. Indeed, in time domain the Gaussian likelihood reads

$$\mathcal{L} \propto \exp \left( -\frac{1}{2} (\mathbf{d} - \mathbf{s})^T E^{-1} (\mathbf{d} - \mathbf{s}) \right), \quad (18)$$

where  $E$  is the covariance matrix for the intrinsic noise of the instrument. For a white noise of variance  $\sigma^2$ ,  $E_{ij} = \delta_{ij}\sigma^2$ . Further,  $\mathbf{d}$  and  $\mathbf{s}$  are data and DM signal vectors composed of elements  $d(t_i)$  and  $s(t_i)$  on the time grid  $\{t_i\}$ . This likelihood simply states that the residuals are consistent with the instrument noise. The Gaussian likelihood is the starting point for developing many practically used data analysis techniques, such as the periodogram and matched filter techniques.

We demonstrate a similar result to Eq. (13) by taking the large limit of  $\gamma$  in the likelihood (18). First, we marginalize over the phase  $\theta$  arriving at

$$\int p(\theta|I) \mathcal{L} d\theta \sim \exp \left( -\frac{x^2}{4} \frac{\Phi_0^2}{\Phi_{\text{DM}}^2} \right).$$

Here we took into account that  $\sum_{i=1}^N \cos^2(2\pi f_\phi t_i + \theta) = N/2$  when averaged over  $\theta$ . For the stochastic case we additionally integrate the above equation over  $\Phi_0$  with amplitude distribution (2) leading to  $p_{\text{det}}(x) \propto \exp(-x^2/4)$  and  $p_{\text{stoch}}(x) \propto \frac{1}{1+x^2/4}$ . As in the main text  $x \equiv \gamma \times \Phi_{\text{DM}} \sqrt{N} \sigma^{-1}$ . These formulas recover the tail behavior of the rigorous DFT results (9,11) and support our claim that in the stochastic treatment, the posterior assumes Lorentzian-like shape slowly decaying as  $\gamma^{-2}$ . Using these approximate posteriors we compute the ratio of  $\gamma_{95\%}$  constraints to be  $\approx 9.2$  consistent with the more rigorous Eq. (13). Moreover, this result holds for the most general case of colored noise and non-uniform time grids, as in this case  $x = \gamma \Phi_{\text{DM}} \times \left[ \sum_{i,j=1}^N (E^{-1})_{ij} \cos(2\pi f_\phi(t_i - t_j)) \right]^{1/2}$ ; this modification does not affect the derived ratio between the widths of the two distributions.

### D. Blueice Monte Carlo

Here we use a method widely used in astroparticle physics [6] to compare to the Bayesian approach above. In the case considered here we construct a model of the signal and the background by simulating the response of the axion field with a given frequency  $\nu_{ax}$ , phase  $\phi_{ax}$  and coupling  $\gamma_{ax}$  to nuclear spins and measuring the NMR response as is done in the CASPER-ZULF experiment [7]. The signal and background models are defined in frequency and Fourier amplitude space and their PDFs are computed by sampling from the simulator. PDFs are computed for different fixed axion amplitudes and interpolated for intermediate values using blueice [3].

The likelihood can then be explicitly written as:

$$\mathcal{L}(\nu_{ax}, \phi_{ax}, \gamma_{ax} | \vec{x}) = \prod_{i=1}^N f(\nu_{ax}, \phi_{ax}, \gamma_{ax}, x_i), \quad (19)$$

where the product is taken over each frequency bin and  $f(x)$  (determined by the simulator) gives the probability of the Fourier amplitude at this frequency for a given signal.

For studying the effect of the amplitude fluctuation we construct two likelihoods. One where the PDFs are constructed by sampling from the simulator without Rayleigh distributed amplitude fluctuations and one case with fluctuations. The inference on both likelihoods is the same. During the construction of the PDFs for the case with amplitude fluctuations, the amplitude  $\gamma_{ax}$  is multiplied by a random draw from the Rayleigh distribution effectively marginalising over this parameter.

Upper limits can then be determined considering the maximum likelihood ratio test statistic:

$$q = \frac{\mathcal{L}(\gamma_{\text{true}} | \vec{x})}{\mathcal{L}(\gamma_{\text{best}} | \vec{x})}. \quad (20)$$

Under certain, but rather generic, conditions confidence intervals and in particular upper limits can be constructed using approximations outlined in Wilks theorem [8], which states that the test statistic (defined in Eq. (20)) is distributed as a chi-squared under above mentioned conditions. In the case encountered here, we find that Wilks

theorem does not hold. In a situation like this, one has to resort to doing a so-called Neyman construction, see e.g. discussion in [9]).

The decisive feature of a Neyman construction is that it provides the statistically desired properties (in this case the coverage of the confidence intervals) per construction.

The correction factor is finally not determined from a single experiment but rather from an ensemble of experiments over which the so called sensitivity (median limit in case of no signal) is calculated. The correction factor is then defined analogous to the case of the Bayesian analysis as:

$$\text{correction} = \frac{\text{median}(u_{\text{stochastic}})}{\text{median}(u_{\text{deterministic}})} \quad (21)$$

where  $u$  is a large number of upper limits at a certain confidence level.

Initial results from the simulations show a correction factor  $\gtrsim 4$ .

## II. RAYLEIGH DISTRIBUTION

As shown in Eq. (1),  $\Phi_0$  is the observed amplitude, and in the case of total interrogation time being much less than the field's coherence time,  $T \ll \tau_c$ , the only amplitude observed during a measurement.

Since everything hinges on the observed dark matter density  $\rho_{\text{DM}}$ , one can relate this to the field's energy density  $\Phi_0^2 f_\phi^2 / 2 = \rho_{\text{DM}}$  as done for example by Graham in [10]. The problem with this is that  $\Phi_0$  is actually a Rayleigh distributed value, thus the correct expression is

$$\langle \Phi_0^2 \rangle \frac{c^2 m_\phi^2}{2\hbar^2} = \rho_{\text{DM}}. \quad (22)$$

We can define  $\Phi_{\text{DM}}$  as the value satisfying Eq. (22)

$$\Phi_{\text{DM}} = \sqrt{\langle \Phi_0^2 \rangle} = \frac{\sqrt{2\rho_{\text{DM}}}}{m_\phi}, \quad (23)$$

analogous to previous assumptions of  $\Phi_0 = \Phi_{\text{DM}}$  in the deterministic approach.

Using Eq. (22) we can solve for the required  $\sigma$  of the Rayleigh distribution  $p(\Phi_0)$ .

$$\begin{aligned} \langle \Phi_0^2 \rangle &= \int \Phi_0^2 p(\Phi_0) d\Phi_0 = \int_0^\infty \frac{\Phi_0^3}{\sigma^2} \exp\left(-\frac{\Phi_0^2}{2\sigma^2}\right) d\Phi_0 = \Phi_{\text{DM}}^2 \\ \implies \sigma &= \Phi_{\text{DM}}/\sqrt{2} \text{ thus,} \\ p(\Phi_0) &= 2 \frac{\Phi_0}{\Phi_{\text{DM}}^2} \exp\left(-\frac{\Phi_0^2}{\Phi_{\text{DM}}^2}\right). \end{aligned} \quad (24)$$

Note that the average value of this distribution  $\langle \Phi_0 \rangle = \Phi_{\text{DM}} \sqrt{\pi}/2$  is not simply  $\Phi_{\text{DM}}$ . Approximately 63% of given field realizations will have an amplitude smaller than  $\Phi_{\text{DM}}$ . The distribution compared to  $\Phi_{\text{DM}}$  is shown in Fig. 1.

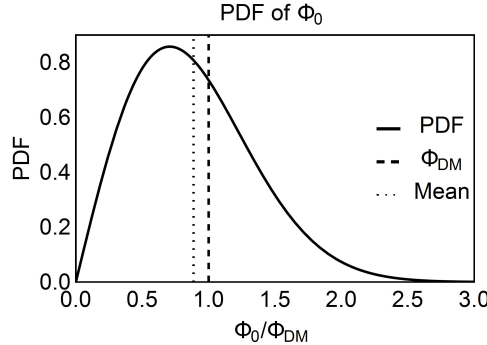


FIG. 1: Rayleigh distribution given by Eq. (24).

- 
- [1] A. Derevianko, Detecting dark-matter waves with a network of precision-measurement tools, *Phys. Rev. A* **97**, 042506 (2018), [arXiv:1605.09717](#).
  - [2] S. Knirck, A. J. Millar, C. A. O'Hare, J. Redondo, and F. D. Steffen, Directional axion detection, *J. Cosmol. Astropart. Phys.* **2018** (11), 051, [arXiv:1806.05927](#).
  - [3] J. Aalbers, K. Dundas Morã, and B. Pelssers, [JelleAalbers/blueice: v1.0.0-beta.2](#) (2019).
  - [4] E. T. Jaynes, Bayesian Spectrum and Chirp Analysis, in *Maximum-Entropy and Bayesian Spectral Analysis and Estimation Problems*, edited by C. R. Smith and G. J. Erickson (D. Reidel Publishing Company, Dordrecht, Holland, 1987) pp. 1–37.
  - [5] Strictly speaking one needs to use Jeffrey's (scale invariant prior)  $\propto 1/\gamma$  here, but the previous analyses do not use it. We employ a sufficiently broad uniform prior for  $\gamma$  for consistency with the literature.
  - [6] J. Conrad, [Statistical issues in astrophysical searches for particle dark matter](#) (2015).
  - [7] A. Garcon, J. W. Blanchard, G. P. Centers, N. L. Figueroa, P. W. Graham, D. F. J. Kimball, S. Rajendran, A. O. Sushkov, Y. V. Stadnik, A. Wickenbrock, T. Wu, and D. Budker, Constraints on bosonic dark matter from ultralow-field nuclear magnetic resonance, [arXiv Prepr. arXiv1902.04644](#) (2019), [arXiv:1902.04644](#).
  - [8] S. S. Wilks, The Large-Sample Distribution of the Likelihood Ratio for Testing Composite Hypotheses, *Ann. Math. Stat.* **9**, 60 (1938).
  - [9] M. Tanabashi, K. Hagiwara, K. Hikasa, K. Nakamura, Y. Sumino, F. Takahashi, J. Tanaka, K. Agashe, G. Aielli, C. Amsler, *et al.*, [Review of Particle Physics](#) (2018), [arXiv:0601168 \[astro-ph\]](#).
  - [10] P. W. Graham and S. Rajendran, New observables for direct detection of axion dark matter, *Phys. Rev. D - Part. Fields, Gravit. Cosmol.* **88**, 1 (2013), [arXiv:arXiv:1306.6088v2](#).